In Situ Studies of the Primary Immune Response to (4-Hydroxy-3-Nitrophenyl)Acetyl IV. Affinity-dependent, Antigen-driven B Cell Apoptosis in Germinal Centers as a Mechanism for Maintaining Self-tolerance

By Shuhua Han, Biao Zheng, Joseph Dal Porto, and Garnett Kelsoe

From the Department of Microbiology and Immunology, University of Maryland School of Medicine, Baltimore, Maryland 21201

Summary

Germinal centers (GCs) are the sites of antigen-driven V(D)J gene hypermutation and selection necessary for the generation of high affinity memory B lymphocytes. Despite the antigen dependence of this reaction, injection of soluble antigen during an established primary immune response induces massive apoptotic death in GC B cells, but not in clonally related populations of nonfollicular B lymphoblasts and plasmacytes. Cell death in GCs occurs predominantly among light zone centrocytes, is antigen specific, and peaks within 4–8 h after injection. Antigen-induced programmed death does not involve cellular interactions mediated by CD40 ligand (CD40L) or Fas; disruption of GCs by antibody specific for CD40L was not driven by apoptosis and C57BL/6.*lpr* mice, though unable to express the Fas death trigger, remained fully susceptible to soluble antigen. Single injections of antigen did not significantly decrease GC numbers or average size, but repeated injections during an 18-h period resulted in fewer and substantially smaller GCs. As cell loss appeared most extensive in the light zone, decreased GC cellularity after prolonged exposure to soluble antigen implies that the Ig^- centroblasts of the dark zone may require replenishment from light zone cells that have survived antigenic selection. GC cell death is avidity-dependent; oligovalent antigen induced relatively little apoptosis and GC B cells that survived long exposures to multivalent antigen expressed atypical VDJ rearrangements unlikely to encode high affinity antibody. Antigen-induced apoptotic death in GCs may represent a mechanism for the peripheral deletion of autoreactive B cell mutants much as the combinatorial repertoire of immature B lymphocytes is censored in the bone marrow.

Germinal centers (GCs)[1] develop in secondary lymphoid tissues after immunization, and they represent oligoclonal clusters of rapidly dividing, antigen-reactive B lymphocytes (1–3). These cells can be identified histologically by their distinctive affinity for the plant lectin, peanut agglutinin (PNA^+) and lack of membrane IgD ($mIgD^-$) (4). This follicular microenvironment also comprises smaller but requisite populations of antigen-specific T helper cells (5–7) and follicular dendritic cells (FDCs) that are specialized for the retention of antigen–antibody complexes (8, 9). Interaction between these cell populations activates V(D)J hypermutation, resulting in the rapid step-wise introduction of point mutations into the variable region of Ig H and L chain genes and in T cell antigen receptor α-chain genes (7–13). Genetic and phenotypic evidence suggest that B cell mutants are selected by competition for antigen, presumably that which is held on the FDC; this selection generally favors higher affinity mutants that survive repeated rounds of mutation and selection to dominate the memory compartment of B lymphocytes (14–18).

The primary GC reaction of C57BL/6 (Igh^b) mice immunized with proteins conjugated with the (4-hydroxy-3-nitrophenyl)acetyl (NP) hapten provides a useful model for examining this complex response (2, 10, 11, 16–18). The B cell response to NP is highly restricted in Igh^b strains: virtually all primary anti-NP antibodies bear the λ1 L chain, share a characteristic idiotype, and are heteroclitic for the NP analogue (4-hydroxy-5-iodo-3-nitrophenyl)-acetyl (NIP) (19, 20). The dominant H chain expressed in this population is encoded by the V_H186.2, DFL16.1, and J_H2 gene segments, and it bears a tyrosine-rich CDR3 associated with robust NP/NIP binding (21, 22).

NP-reactive, $\lambda1^+$ GCs first appear in the spleen on day 4

[1] *Abbreviations used in this paper.* AP, alkaline phosphatase; CD40L, CD40-ligand; CGG, chicken γ-globulin; CVF, cobra venom factor; FDC, follicular dendritic cell; GC, germinal center; HRP, horseradish peroxidase; mIg, membrane Ig; NIP, (4-hydroxy-5-iodo-3-nitrophenyl)acetyl; NP, (4-hydroxy-3-nitrophenyl)acetyl; PALS, periarteriolar lymphoid sheath; PNA, peanut agglutinin; TUNEL, terminal deoxynucleotidyl transferase-mediated dUTP-biotin nick-end labeling.

of the response, and they persist for ~3 wk (2, 23, 24). V(D)J hypermutation is not active during the early proliferative phase of GC development; Ig mutations are first observed 7–8 d after immunization (11, 24), coincidentally with increased expression of the B7-2 molecule within the GC light zone (25). Before day 8, GC B cell populations are clonally diverse, and lymphocytes expressing V_H186.2 rearrangements are not dominant (24). In early (day 4–6) $\lambda1^+$ GCs, the most frequent VDJ rearrangements contain the C1H4, V23, and CH10 V_H exons (24). These gene segments share a high degree of sequence similarity with the V186.2 gene, and they can encode $\lambda1^+$ antibodies that bind NP (26–28). When expressed by transfection, however, these antibodies generally possess lower affinities for NP/NIP than do those encoded by the canonical VDJ (reference 29 and Dal Porto, J., and G. Kelsoe, unpublished data). By day 8 of the response, these atypical cells become infrequent (~5%) in GCs, presumably as a consequence of antigen-driven competition (24).

An undesirable consequence of V(D)J hypermutation is the generation of autoreactive lymphocytes (30–32). Although the ability to sustain self-reactive mutants is diminished by the reciprocal oligoclonality of GC T- and B cells (33), we and others have developed experimental models to study the fate of GC B cells that acquire specificity for an abundant self antigen present within the splenic compartment. Recently, Pulendran et al. (34) and Shokat and Goodnow (35) demonstrated antigen-specific cell death in normal and transgenic GC B lymphocytes after the injection of soluble antigen. This cell death was characterized by the rapid DNA fragmentation of apoptosis, but was only slightly impeded or completely resistant to constitutive expression of the antiapoptotic protooncogene *bcl-2*. While neither of these groups could assign a specific mechanism to GC apoptosis, Pulendran and his colleagues concluded that antigen most likely acted directly on GC B cells. Here we show that in C57BL/6 mice immunized with NP conjugated to chicken γ-globulin (NP_{12}-CGG), GCs arise which contain $\lambda1^+$ B cells that rapidly undergo apoptosis after the injection of soluble proteins bearing the NIP hapten. Apoptosis was confined to GC B cells, and was antigen specific and avidity dependent. Abrogation of cellular interactions mediated through the CD40 ligand (CD40L) resulted in the rapid loss of splenic GCs by migration rather than by cell death, suggesting that free antigen does not act by disrupting lymphocyte collaboration signals. C57BL/6.MRL*lpr* mice remained susceptible to antigen-induced apoptosis, demonstrating the independence of programmed cell death from the Fas molecule. Interestingly, prolonged administration of soluble antigen resulted in the cellular depletion of GCs by sustained apoptosis and selected for a residual population of atypical, presumably low affinity B cell mutants, reversing the usual direction of B lymphocyte evolution.

Materials and Methods

Antigens and Immunizations. The succinic anhydride esters of NP or NIP (Cambridge Research Biochemicals, Cambridge, UK) were reacted with CGG (Accurate Scientific, Westbury, CT) or BSA (U.S. Biochemical Corp., Cleveland, OH) as described (2); hapten/protein ratios were determined spectrophotometrically. All mice were immunized with a single i.p. injection of 50 μg NP_{12}–CGG precipitated in alum. Cobra venom factor (CVF) (20 U; Quidel, San Diego, CA) was given i.p. 30 min before the injection of soluble NIP–protein to decomplement mice by C3 depletion. Isoproterenol hydrochloride (Sigma Chemical Co., St. Louis, MO) was injected (150 μg/kg body wt) concurrently with NIP–protein to prevent anaphylactoid reactions. Soluble NIP–protein conjugates were administered 9 d after immunization in a single i.p. injection of 4 mg antigen in a 0.5-ml vol of PBS. Some mice received multiple i.p. injections of soluble NIP_{12}–CGG on day 9; 4 mg protein was injected initially and 2 mg was given 6, 12, and 18 h later. These animals were killed 2 h after the final injection of soluble antigen.

Histology. Spleens were prepared for histology as described (2). Splenic cell populations were visualized by immunocytochemical labeling with antibodies or PNA conjugated with biotin, horseradish peroxidase (HRP), or alkaline phosphatase (AP) (2). Bound HRP and AP activities were located by reacting the labeled section with 3-aminoethyl carbazole and napthol AS-MX phosphate/Fast Blue BB (Sigma), respectively. Bound biotinylated antibody or lectin was visualized with HRP or AP conjugates of streptavidin (Southern Biotechnology Associates, Birmingham, AL). PNA-HRP and PNA–biotin were obtained from E-Y Laboratories (San Mateo, CA); biotinylated antibodies specific for mouse IgD or B220 were purchased from Southern Biotechnology and Pharmingen (San Diego, CA), respectively; Ls136, GK1.5, and MR1 antibodies, specific for mouse λ1 light chain, mouse CD4, and mouse CD40L, respectively, were produced in vitro and purified by elution from protein A. Terminal deoxynucleotidyl transferase (Tdt)-mediated dUTP-biotin nick-end labeling (TUNEL) was used to identify apoptotic cell nuclei (36) (Apoptag; Oncor, Gaithersburg, MD). Sections with $TUNEL^+$ cells were counterstained either with hematoxylin and eosin, or were colabeled with antibodies or PNA.

$TUNEL^+$ cells were counted at a magnification of 200 by systematic scanning of the entire section. Counts were confirmed by blinded recounts; independent duplicate counts varied by ≤15%.

Amplification and Sequencing of VDJ DNA from GC B Cells. Cellular material representing ~20 $TUNEL^-$ GC B cells was microdissected from single $\lambda1^+$ GCs as described and subjected to two rounds of PCR amplification (23, 24) driven by the *Pfu* thermostable polymerase (7). Amplified VDJ fragments were ligated into the plasmid pBSK II to transform bacteria, and inserts obtained from single bacterial colonies were sequenced in both directions (23, 24). The measured error rate of the *Pfu* polymerase is $1–2 \times 10^{-6}$ misincorporations/bp per cycle, resulting in two to three artifactual mutations per 100 VDJ clones (7). This frequency is sufficiently low to permit the assumption that all recovered mutations represent in vivo events.

Results

Anaphylactoid Reactions Follow the Injection of Soluble Antigen. Though previously unreported (34, 35), our initial experiments were complicated by frequent and severe anaphylactoid reactions triggered by the formation of immune complexes (37). Injection of equivalent amounts of BSA alone or irrelevant hapten conjugates produced no response. Physiologic shock became obvious within 5 min after the

injection of soluble antigen, and it resulted in ~20% mortality. These reactions persisted even after decomplementation with CVF (38), but they were blocked by administering the β-agonist isoproterenol (39, 40) concurrently with soluble NIP–protein. Administration of CVF and/or isoproterenol had no discernable effect on the splenic histology or numbers and distribution of apoptotic cells in immune control mice or in those receiving soluble NIP–protein (not shown). Thus, subsequent experiments were carried out in mice that had received isoproterenol to minimize the anaphylactogenic effect of immune complexes. Pairwise analysis (Student's *t* test) of induced apoptosis in each group (antigen, antigen + CVF, antigen + isoproterenol, antigen + CVF, + isoproterenol) revealed no statistically significant ($P > 0.05$) differences, thus data from all experiments have been pooled.

Histology and Kinetics of Antigen-induced Apoptosis in Germinal Centers. Spleens of control mice that did not receive soluble NIP–protein exhibited typical and vigorous immune responses with large collections of extrafollicular plasmacytes and prominent PNA^+ GCs (Fig. 1 *A*). Low numbers of apoptotic cells ($TUNEL^+$) were identified within normal GCs (Fig. 1 *A*), and only rarely within the periarteriolar lymphoid sheaths (PALS) or splenic red pulp. By day 9 of the primary anti-NP response, collections of lymphoblasts and plasmacytes form large foci of NP/NIP–binding cells with abundant cytoplasmic Ig. These foci are located at the periphery of the PALS, and occasional $\lambda 1^+$ plasmacytes are scattered throughout the red pulp (2). Although these cells are specialized for antibody production and are excluded from the memory compartment (2, 23, 41), they are clonally related to adjacent GC B cell populations (23). Absence of $TUNEL^+$ cells within the PALS and red pulp suggests that GC apoptosis is solely the consequence of that particular microenvironment. Within GCs, the majority of $TUNEL^+$ cells/nuclei were contained within tingible body macrophages as clumps of two to five cells per nuclei (Fig. 1 *A*). Some of these apoptotic cells could be colabeled by an antibody specific for the B cell marker, B220 (not shown).

In contrast, after injecting NIP_{15}–BSA, the numbers of $TUNEL^+$ cells increased dramatically in GCs, but not elsewhere in the spleen (Fig. 1 *B*). Apoptotic cells were most frequent in the GC light zone (Fig. 1 *B*) and were usually clustered in groups of ≥10 cells (Fig. 1 *C*). Clustering probably represents engulfment by macrophages, although we could not demonstrate the presence of a tingible body macrophage in every section. Despite this large wave of induced cell death, the numbers and cross-sectional area of GCs remained relatively constant during the 18 h of study, presumably because of the continued migration of mIg^- centroblasts from the dark zone (42).

The apoptosis induced by soluble antigen was rapid; by 3 h after injection, the number of $TUNEL^+$ GC cells rose significantly above background levels, reaching a peak of ~55 apoptotic cells per follicle at 5 h, and eventually declining to normal levels by 18 h (Fig. 2). Antigen-induced apoptosis was sensitive to hapten density. Injection of NIP_4–BSA resulted in a maximum increase in $TUNEL^+$ GC cells (~28 apoptotic cells per follicle) that was about one-half of that observed with the more heavily substituted NIP_{15}–BSA. Injection of an equal amount of soluble BSA had no effect on the splenic histology or the frequency of $TUNEL^+$ cells (Fig. 2). Thus, GC cell death was antigen specific and proportional to ligand density.

Soluble Antigen Does Not Initiate Programmed Cell Death by Disrupting T–B Cell Collaboration. In GCs, both the B and T cell populations are specific for the immunizing antigen (1–3, 5–7). The effects of NIP–BSA could therefore result from interference in cognate T–B interaction; hapten-specific B cells presenting processed BSA fragments would be

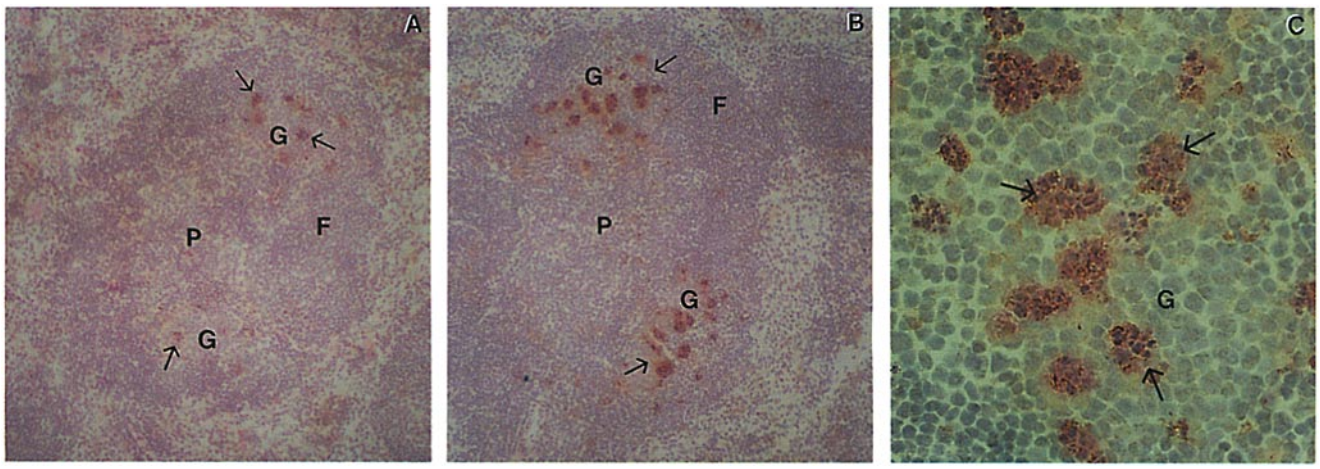

Figure 1. Antigen-induced apoptosis in splenic GCs. On day 9 of a primary immune response to NP_{12}-CGG/alum, the spleens of control immune C57BL/6 mice (*A*) contained well-formed GCs (*G*) within the lymphoid follicles (*F*) of the white pulp. These GCs contained low numbers of $TUNEL^+$ cells (*arrows*), ~20 apoptotic nuclei per follicle, which were generally located distally from the PALS (*P*). In contrast, 5 h after injecting 4 mg of soluble NIP_{15}-BSA (*B*), the frequency of $TUNEL^+$ cells in splenic GCs increased significantly, to ~60 per follicle. These apoptotic cells were generally clustered (*C*), probably because of engulfment by tingible body macrophages. Sections were labeled by the TUNEL method (14) and then counter-stained with hematoxylin and eosin. *A* and *B*, ×100; *C*, ×400.

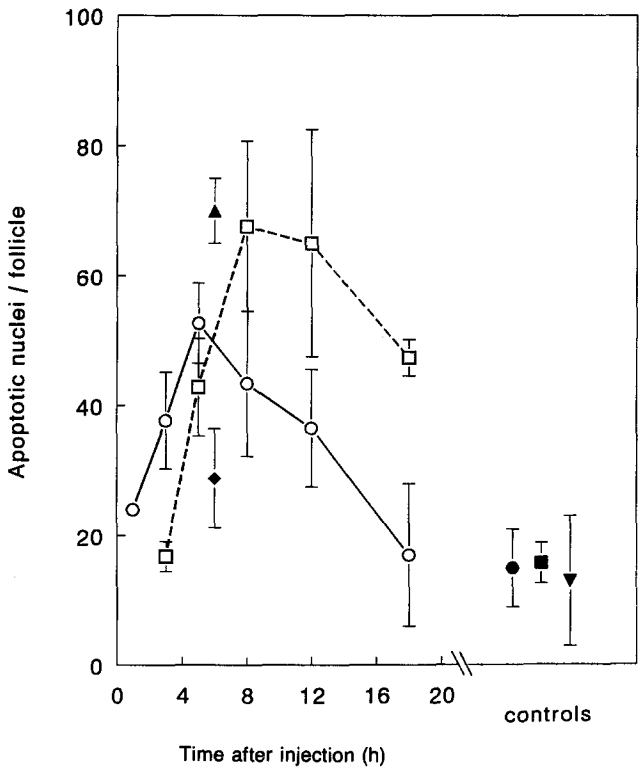

Figure 2. Kinetics of antigen-induced GC apoptosis in C57BL/6 and C57BL/6.*lpr* mice. On day 9 of a primary response to NP_{12}-CGG, C57BL/6 mice were injected i.p. with 4 mg NIP_{15}-BSA (○) or NIP_{12}-CGG (□) plus CVF (20 U) and isoproterenol (150 μg/kg). Control mice either received CVF and isoproterenol alone (■) or 4 mg BSA (●). Mice were killed at the times indicated; BSA controls (●) were studied 6 h after injection. Spleens were prepared for histology, and apoptotic nuclei were labeled as for Fig. 1; $TUNEL^+$ cells were enumerated at ×200 in two to three sections per spleen. Results from four independent experiments (n = 2–11) have been averaged (±SEM). Injection of NIP_{15}-BSA (○) or NIP_{12}-CGG (□) induced large increases in the numbers of $TUNEL^+$ cells/nuclei per follicle. Apoptosis was elevated slightly above background levels (■) by 3 h after injection, and it reached maximum levels at 5–8 h. Antigen treatment did not result in the loss of splenic GCs, and by 18 h after injection, the frequency of follicular apoptotic cells returned to nearly normal levels. Injection of BSA (●) did not result in increased numbers of $TUNEL^+$ cells, and 6 h after the injection of 300 μg of MR1 antibody (◆), only a modest increase in the number of apoptotic cells was observed. Fas^- C57BL/6.*lpr* mice (▲) were fully susceptible to antigen-induced apoptosis, demonstrating that cell death is independent of FasL: Fas cross-linking (17). Interestingly, $TUNEL^+$ cells were present at normal levels in control immune C57BL/6.*lpr* mice (▼).

unable to collaborate with CGG-specific T cells. To test this possibility, we injected soluble NIP_{12}–CGG on day 9 and determined the frequency of $TUNEL^+$ cells as before. Fig. 2 illustrates that NIP_{12}–CGG induced apoptosis in GCs with kinetics similar to that caused by NIP_{15}–BSA. Indeed, the number of apoptotic cells per follicle in mice treated with NIP_{12}–CGG was greater (~70 apoptotic cells per follicle) than that found in mice receiving NIP_{15}–BSA. This increase represents death of both NIP- and CGG-specific GC B cells (2), but did not result in the elimination of splenic GCs. Thus, a soluble NIP–protein conjugate that could be recognized by collaborating T helper cells within the GCs induced apoptotic death as effectively as the heterologous NIP–BSA conjugate. This finding suggests that soluble antigen does not block cognate T cell help, but induces GC B cell death directly, or possibly by interfering with B–FDC interaction.

Additional experiments were performed to test the conclusion that antigen-induced apoptosis is not mediated through T–B cell contact. The CD40L expressed on activated T cells is necessary for the GC reaction (43, 44), and injection of the anti-CD40L antibody, MR1, disrupts established GCs within 24 h (25). To establish if this effect is driven by apoptosis and shares the kinetics of antigen-induced cell death, immunized mice were injected with 300 μg of MR1 antibody instead of soluble antigen. To our surprise, MR1 antibody did not abrogate the GC reaction by inducing programmed cell death, but rather, it appeared to initiate GC B cell migration from the lymphoid follicle. Before the administration of anti-CD40L antibody, GCs were abundant and contained normal levels of apoptotic cells (Fig. 3 *A*). By 6 h after the administration of MR1, the frequency of apoptotic cells rose modestly, reaching a maximum comparable to that seen early (3 h) after injection of NIP–protein (Figs. 2 and 3 *B*). Higher doses of MR1 antibody (600 μg) elicited similar migrations (not shown). Thus, disruption of T–B interaction through the CD40L is relatively ineffective in causing GC cell death. Injected MR1 antibody, however, did exert a powerful effect on GC B cells, since PNA^+ GCs were virtually absent in the spleens of MR1-treated animals at 12–18 h after injection (Fig. 3 *C*). This loss did not represent downregulation of the PNA-binding phenotype, since staining with anti-IgD antibody revealed no substantial collections of IgD^-, $B220^+$ cells remaining within the lymphoid follicles. This role for CD40L in maintaining GC integrity was unexpected and may represent failure to replenish the dark zone by recirculating centrocytes (3, 45). Although our experiments do not permit a detailed accounting of MR1-induced GC cell migration, at least some IgD^-, $B220^+$ migrants enter the PALS.

Fas-independent Apoptosis in Germinal Center B Cells. T helper cells can cause apoptotic death by cross-linking the Fas molecules that are expressed on the surface of activated B lymphocytes (46–48). Mice homozygous for the *lpr* mutation poorly express Fas, and their lymphocytes are resistant to this pathway of programmed cell death (49–51). C57BL/6 mice congenic for the *lpr* locus were fully susceptible to antigen-induced cell death (Fig. 2), further supporting the T cell independence of this event. Interestingly, the number of apoptotic cells per follicle in C57BL/6.MRL-*lpr* mice that did not receive soluble antigen fell within the range observed for normal C57BL/6 animals (Fig. 2), indicating that Fas-independent cell death normally occurs in GCs.

Prolonged Exposure to Soluble Antigen Enriches Germinal Centers for Atypical V_H Genes. Persistence of GCs in the face of antigen-induced apoptosis suggested that the Ig^- centroblasts in the dark zone continued to replenish the light zone centrocytes during the study period (42). Ig^+ centrocytes emerging after the elimination/reduction of free antigen by serum antibody could then continue the GC reaction. To test this possibility, a group of immune mice were given in-

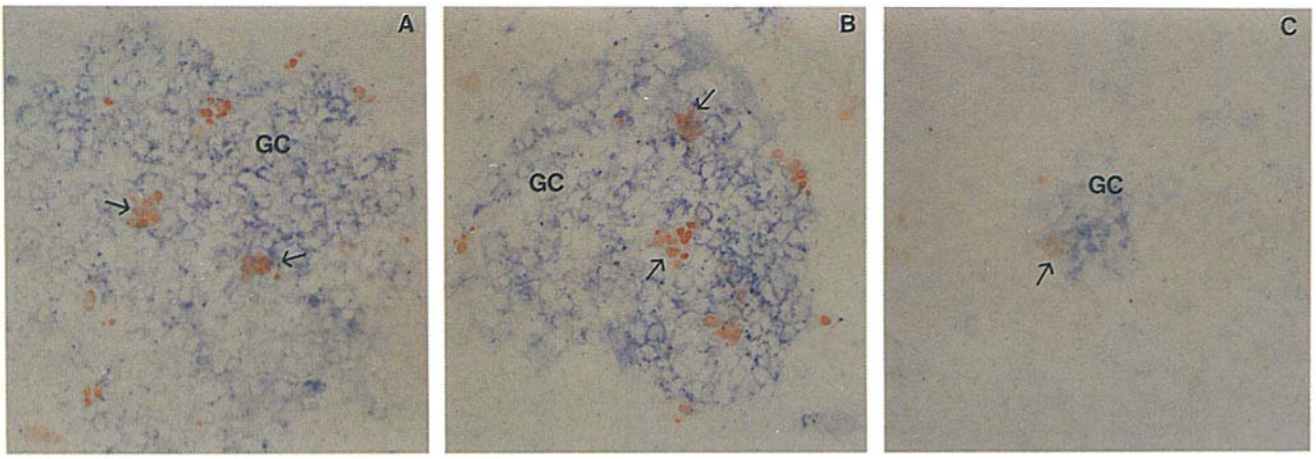

Figure 3. The anti-CD40L antibody, MR1, disrupts established GCs by cell emigration. 9 d after primary immunization with NP_{12}-CGG (*A*), splenic GCs consist of large clusters of PNA^+ B cells (*blue*) that contain scattered collections of apoptotic nuclei (*red*, *arrows*) usually within tingible body macrophages. 6 h after injecting 300 μg of MR1 antibody (*B*), the number of $TUNEL^+$ cells within the GC is modestly increased but otherwise the splenic histology appears unchanged. By 12 h after injection (*C*), however, only occasional collections of PNA^+ cells remain in the lymphoid follicles. Sections were labeled by the TUNEL method (14) to identify apoptotic cells, and they were then incubated with PNA-biotin/streptavidin-AP (10) to label GCs (2). ×200.

jections of NIP_{12}–CGG at 6-h intervals (0, 6, 12, and 18 h); 2 h after the final injection, the spleens of treated mice were taken for histology. The effects of prolonged administration of antigen were consistent with specific and avidity-dependent depletion of Ig^+ centrocytes. At 20 h, the number of splenic GCs in antigen-treated mice was reduced by a nonsignificant amount from that in immune controls (average = 38 vs. 45 per section), but their average area was only 20–25% of control GCs (Figs. 4, *A* and *B*), indicating a four- to fivefold reduction in cellularity. These small GCs contained relatively few $TUNEL^+$ cells (Fig. 4 *C*), suggesting resistance to continued antigen-induced apoptosis.

Resistance to apoptosis could reflect altered cell physiology, e.g., reactivation of the *bcl-2* or *bcl-x* genes (52, 53), or expression of mIg with low affinity for antigen. To determine if the B cell populations that survived prolonged administration of soluble NIP–CGG expressed canonical, high affinity VDJ rearrangements, ~20 $TUNEL^-$ cells were microdissected from remanent $\lambda 1^+$ GCs; endogenous VDJ fragments were then amplified from the recovered genomic DNA by a PCR for cloning and DNA sequencing (7, 23, 24). 15 VDJ fragments recovered from three randomly chosen GCs are shown in Fig. 5. Only three of the recovered VDJ sequences represented canonical $V_H186.2$/DFL16.1 associations (S1AB01.1–S1AB01.3). Another five sequences (S1AB02.1–S1AB02.5) consisted of $V_H186.2$ joined to DSP.2 and the remaining seven fragments contained the noncanonical C1H4 (S1AB03.2, S1AB03.3, S1AB03.5,), V23

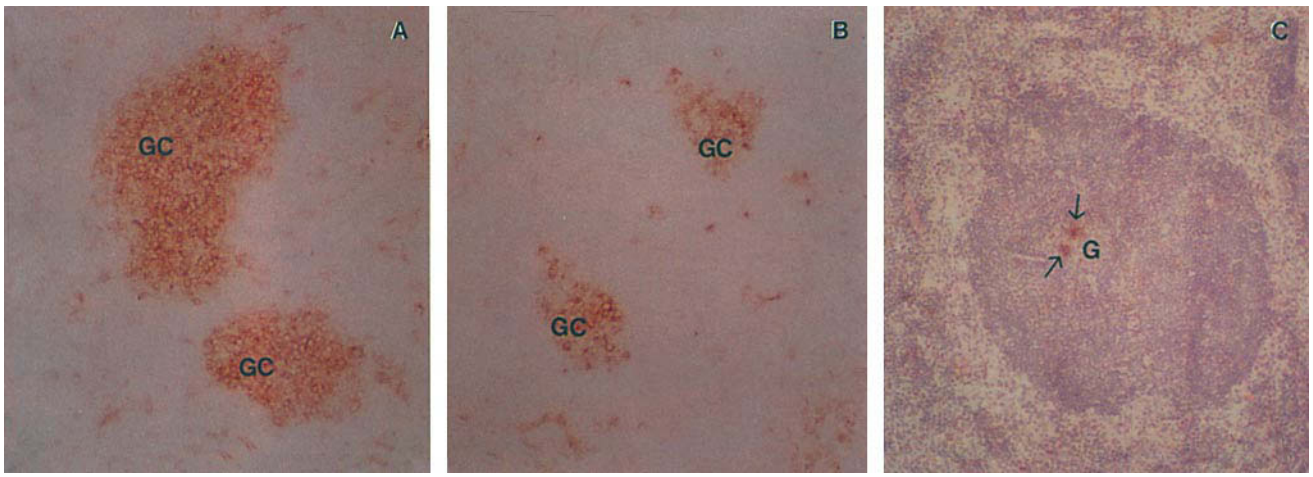

Figure 4. Prolonged administration of soluble antigen depletes GC populations. mIg^- centroblasts divide every 7–10 h (2, 3, 42) to produce the Ig^+ centrocytes of the GC light zone. Concentrations of circulating NIP_{12}-CGG were maintained for approximately two centroblast doublings (18 h) by repeated i.p. injections. In contrast to a single administration of soluble antigen (see Fig. 1 *B*), repeated injections of antigen significantly reduced the area of splenic GCs (*B*) compared with controls given equivalent amounts of BSA (*A*). The average reduction in GC area was to 20–25% of that seen in controls, indicating a four- to fivefold decrease in cellularity. After 20 h of exposure to soluble antigen, the frequency of $TUNEL^+$ GC cells is reduced to normal levels (*C*). For comparison to apoptosis in normal GCs and after a single injection of NIP-BSA, see Fig. 1. *A* and *B*, ×200; *C*, ×100.

Clone	20	31	33	34	46	53	62	65	71	72	76	81	CDR3							J_H				
S1AB01.1	---	---	TGG→TGC (Trp→Cys)	ATG→ATT (Met→Ile)	GAG→GAC (Glu→Asp)	---	---	---	---	---	AGC→AGT (Ser)	---	ACG (Thr)	TAT (Tyr)	TAC (Tyr)	TAC (Tyr)	GGT (Gly)	AGT (Ser)	ATC (Ile)	TAC (Tyr)			GAC	TAC	TGG	V186.2/DFL16.1/J_H2
S1AB01.2, S1AB01.3	CTG→TTG (Leu)	AGC→AGT (Ser)	---	---	---	---	---	AGC→AAC (Ser→Asn)	GTA→GTT (Val)	---	---	---		TAT (Tyr)	TAC (Tyr)	TGC (Cys)	GGT (Gly)	AGT (Ser)	AGC (Ser)		TAC	TTT	GAC	TAC	TGG	V186.2/DFL16.1/J_H2
S1AB01.4, S1AB01.5	---	---	---	---	---	---	---	---	---	---	---	---		CTA (Leu)	GCT (Ala)	GGG (Gly)	ACC (Thr)						GAC	TAC	TGG	CH10/DQ52/J_H2
S1AB02.1- S1AB02.5	---	---	---	---	---	AAT→TAT (Asn→Tyr)	---	AGC→ACC (Ser→Thr)	---	GAC→GTC (Asp→Val)	---	CAG→CAA (Gln)		TAT (Tyr)	GGT (Gly)	AAC (Asn)	TAC (Tyr)	AAG (Lys)		TAC	TTC	GAT	GAC	TGG	V186.2/DSP2.5/J_H1
S1AB03.1, S1AB03.4	---	---	---	---	---	---	AAG→AAC (Lys→Asn)	AGC→AAC (Ser→Asn)	---	---	---	---		AAT (Asn)	TGT (Cys)	AAC (Asn)	TTC (Phe)								TGG	V23/DSP2.7/J_H2
S1AB03.2, S1AB03.3 S1AB03.5	---	---	---	---	---	---	---	---	---	---	---	---	GTG (Val)	GGT (Gly)	GAT (Asp)	TAC (Tyr)	GAC (Asp)	GGG (Gly)	GTT (Val)				GAC	TAC	TGG	C1H4/DSP2.2/J_H2

Figure 5. VDJ fragments recovered from GCs remaining after prolonged administration of soluble antigen. Approximately 20 TUNEL$^-$, PNA$^+$ cells were microdissected from three $\lambda1^+$ splenic GCs (S1AB01, S1AB02, and S1AB03) present in a C57BL/6 mouse that had received four injections of soluble NIP_{12}–CGG during an 18-h period. Recovered genomic DNA was amplified in a two-step PCR using the *Pfu* polymerase. The measured error rate of this heat-stable polymerase is $1–2 \times 10^{-6}$ mutations/bp per cycle (7). Approximately 0.03 artifactual mutations per VDJ sequence are expected from polymerase errors. Five cloned VDJ fragments were sequenced from each GC. V_H exon sequences were defined according to Gu et al. (54), and they are identified with their associated D and J_H elements (far right). All sequences are compared to the appropriate germline element; only those codons that differ from the reference sequences are shown; dashes indicate sequence identity. Amino acids encoded by reference and mutant codons are given in three letter code beneath each mutated codon (ref. → mutant). Silent mutations are indicated by a single amino acid code. Eight of the recovered VDJ fragments represented rearrangements of the V186.2 V_H exon (S1AB01.1–S1AB01.3 and S1AB02.1–S1AB02.5). The remaining seven VDJ fragments contained the C1H4 (S1AB03.2, S1AB03.3, and S1AB03.5), V23 (S1AB03.1 and S1AB03.4), and CH10 (S1AB01.4, and S1AB01.5) V_H exons. The FL16.1 D element was used in association only with three V186.2 rearrangements (S1AB01.1–S1AB01.3); the most common D segment was DSP2, which was present in 10 out of 15 rearrangements. It should be noted that although our PCR primers are designed to amplify J_H2 rearrangements specifically, we occasionally recover VDJ fragments representing VD joins to J_H1 (S1AB02.1–S1AB02.5). Such promiscuous amplification occurs only in GC populations that do not contain a competing J_H2 rearrangement, and they constitute ~3% of our aggregate data set. The DNA sequences recovered in this study are available from GenBank under accession numbers U34979–U34984.

(S1AB03.1 and S1AB03.4), and CH10 (S1AB01.4 and S1AB01.5) V_H exons (54). Mutated V_H gene segments were recovered from all GCs (Fig. 5). Mutations were present in all V186.2 rearrangements at equal frequencies (~1/73 bp) and in two of seven VDJ fragments containing noncanonical, analogue V_H exons. Of the 14 mutations identified, eight (57%) were sited at the AGY sequence motifs characteristic of Ig hypermutation hotspots (55). The frequent recovery of atypical V_H genes and V/D associations from these GCs is unusual; at this time, noncanonical VDJ fragments are only occasionally (~5%) found in the splenic GCs of animals not receiving soluble antigen (24).

The low frequency of canonical V_H186.2 rearrangements in surviving GCs and the poor efficacy of NIP_4–BSA suggest that antigen-induced apoptosis occurs predominantly in higher affinity B cell populations. Usually rare in day 10 GCs, the C1H4, V23, and CH10 analogue V_H genes made up nearly one half (7/15) of the VDJ fragments recovered after 20 h of exposure to soluble antigen. Of those rearrangements containing the V_H186.2 gene segment, only a single example, S1AB01.1, encoded the YYY(GS) CDR3 residues associated with robust NP/NIP binding (22). Significantly, this sequence also contains an unusual Trp→Cys replacement mutation in codon 33 that has not been observed in NP-reactive hybridomas (14, 17, 18, 21, 22, 28, 56–58) or recovered in earlier studies of GC cells (10, 11, 23–26). Position 33 is an important antigen-contacting residue within CDR1 (59).

Discussion

GCs are complex antigen-dependent microenvironments that are necessary for the generation of B cell memory. Antigen-driven hypermutation of Ig V region genes drives the clonal evolution of GC B cells responsible for the increased affinity of antibody produced by memory B lymphocytes (10, 11, 13–18), but it can also generate autoreactive clones (30–32). To determine the fate of GC B cells that acquire specificity for a soluble antigen present in the splenic compartment, we made use of the clonally restricted, heteroclitic antibody response of C57BL/6 mice to the NP hapten (19–22). These mice make a primary set of anti-NP antibodies that use the $\lambda1$ L chain and a canonical H chain encoded by the V186.2 V_H exon joined to DFL16.1; this antibody exhibits ~10-fold higher affinity for the related hapten, NIP. Capitalizing on this heteroclicity, we immunized C57BL/6 mice with NP-CGG and allowed the GC reaction to become established. On day 9 of the response soluble NIP–protein conjugates were injected, allowing the higher affinity NIP ligand to compete with the NP hapten displayed on FDCs for the mIg of GC B cells.

These experiments confirm a novel apoptotic pathway for GC B cells recently described in normal and transgenic mice (34, 35). Soluble NIP conjugates induced extensive cell death within GCs, especially among the mIg$^+$ centrocytes of the light zone (Fig. 1). The onset of apoptosis was rapid (the number of TUNEL$^+$ cells peaked by 4–8 h after the injection of soluble antigen) and was receptor specific in that ligands unrelated to the GC reaction had no effect (Fig. 2).

The possibility that NIP–protein conjugates induced GC apoptosis by interfering with antigen-specific collaboration was tested by administering soluble NIP–CGG. This ligand, homologous to the NP–CGG immunogen used to elicit the GC reaction, could be recognized by both T and B cells in GCs (5–7), but remained an effective inducer of apoptosis

(Fig. 2). Injection of an anti-CD40L antibody at doses that prevent cognate T–B interaction (44) and terminate established GCs (25) induced levels of GC apoptosis only slightly above that seen in control animals (Fig. 2). Together, these observations support the conclusion of Pulendran et al. (34) that this pathway of GC apoptosis is a direct consequence of soluble antigen binding to the murine Ig of GC B cells (34), perhaps in the absence of an ancillary signal(s) provided by the FDC.

Although blockade of cellular interactions mediated by CD40L did not result in substantial GC apoptosis, it did cause the abrupt termination of the GC response, confirming our earlier observations (25). In vivo, passive anti-CD40L antibody appears to disrupt GCs by inducing cellular emigration (Fig. 3). This activity was unexpected from in vitro studies of human tonsil GC cells (52). It may be that the loss or reduction of CD40L expression in GCs normally serves to end the GC reaction by causing memory B cell precursors to leave for other tissue sites. Interestingly, it is now possible to halt the GC reaction at precise times after immunization by injecting anti-CD40L antibody and thus investigate the tempo of evolution in the B cell memory compartment (Dal Porto, J., S. Han, and G. Kelsoe, unpublished data).

Soluble antigen induced apoptosis in GC cells equally well in C57BL/6 and C57BL/6.MRL*lpr* mice, demonstrating that cell death does not require the Fas molecule (Fig. 2). Fas (CD95) is a member of the tumor necrosis factor/nerve growth factor receptor family (60); the cytoplasmic region of Fas contains a motif known as the death domain (61) that is similar to reaper, a small *Drosophila* protein expressed in cells entering apoptosis (62). Signaling through Fas leads to rapid cell death that is only partially inhibited by overexpression of Bcl-2 (63), a phenotype observed in GC apoptosis (34, 35). Fas expression is increased on activated lymphocytes (60), including GC B cells (reference 64 and our unpublished observations), and is thought to play an important role in the regulation of both productive (46–49) and nonproductive (65) immune responses. Nevertheless, Fas does not appear to mediate antigen-induced GC apoptosis. Significantly, the numbers and distribution of TUNEL$^+$ nuclei/cells in the GCs of C57BL/6.MRL*lpr* mice were identical to that observed in normal controls (Fig. 2). This observation indicates that at least some component of GC apoptosis in untreated animals is Fas independent.

Although cell death is extensive, GCs appear little changed after a single injection of NIP–protein. This observation suggests that not all GC B cells are eliminated and/or that the proliferating centroblasts within the GC dark zone are insensitive to soluble antigen and continue to renew the depleted centrocyte population (42). Indeed, repeated injections of soluble antigen during an 18-h period reduced GC cellularity four to fivefold (Fig. 3). This interval corresponds to the time required for two to three doublings of GC centroblasts (2, 3, 42), and it is consistent with exhaustion of the GC dark zone population by their continued recruitment into the light zone, differentiation into mIg$^+$ centrocytes, and subsequent apoptosis. Should the depletion of dark zone cells take place in this manner, centroblasts themselves must be replenished by returning centrocytes in accordance with the model of Kepler and Perelson (45). Cyclic migration between the two poles of the GC with distinct locales for hypermutation and receptor selection provides a useful model for the stepwise accumulation of large numbers of mutations in functional V(D)J rearrangements and the rapid selection for higher affinity mutants (45).

Prolonged administration of soluble antigen, even if homologous to the eliciting immunogen, does not eliminate GCs, but instead, leaves a small B cell population that appears relatively insensitive to antigen-induced apoptosis (Fig. 4 *C*). While these persistent cells could represent a population(s) intrinsically resistant to programmed cell death, they express atypical antigen receptors that are likely to bind NP/NIP with low affinity. Sequence analysis of VDJ fragments recovered from splenic GCs that resisted multiple injections of soluble antigen indicated strong selection against the canonical V186.2/DFL16.1 H chain rearrangement (Fig. 5) that is characteristic of NP-reactive GCs after day 7 of the primary response (11, 24). In fact, in 15 VDJ rearrangements recovered from three GCs, only a single V186.2 rearrangement (Fig. 5, *S1AB01.1*) contained the CDR3 motif YYY(GS), which is typically found in primary anti-NP hybridomas and is important for high affinity binding of the NP and NIP haptens (22, 28). Significantly, this sequence also contained an unusual Trp→Cys replacement in codon 33 that is likely to reduce the affinity of the antigen-combining site for NIP. Position 33 is an important contact residue within CDR1 that mediates 12–15 van der Waals contacts between the NP–NIP ligand and the third hypervariable loop of the canonical H chain (59). This residue is critical for the heteroclitic behavior of the anti-NP antibodies of *Igh^b* mice (59), and a recurrent Trp→Leu mutation in codon 33 increases affinity for NP/NIP ~10-fold (17,18). Replacement of this critical residue by Cys could reduce the number of interactions between the antigen-combining site and the NIP ligand both directly (a modest effect) or indirectly, by altering the position of another important contact residue, Arg 50 (a very strong effect) (reference 59 and Amzel, M., personal communication). We are in the process of generating transfectomas to measure the affinity of λ1 antibodies encoded by the unusual H chain genes that resist antigen-induced apoptosis (29).

Thus, the presence of soluble antigen seems to reverse the usual direction of evolution within GC B cell population. Although resistant cells carry nucleotide substitutions (Fig. 5) typical of Ig hypermutation (55), those that survived 20 h of exposure to free antigen appear selected for decreased antigen affinity. If this pathway of cell death normally serves to eliminate self-reactive lymphocytes arising as a consequence of V(D)J hypermutation (34, 35), then at least two powerful selective forces drive the evolution of memory B cells. Mutants that bind the immunogen with increased affinity exhibit a selective growth advantage within the GC microenvironment; however, should this maturing

affinity introduce self-reactivity, the benefit of this positive selection may be reduced or lost. This developmental boundary could result in evolutionary trajectories that are probable for only a few V_H and V_L pairings.

Finally, this GC death program is remarkably similar to receptor-driven death in immature/transitional B cells (66–68). In sheep, Peyer's patch GC B cells undergo antigen-independent V(D)J hypermutation indistinguishable from that observed in unselected murine κ transgenes (69). This developmentally regulated post-V(D)J diversification illustrates the potential of this special GC microenvironment to function as a primary lymphoid tissue. It may be that the sharing of many phenotypic characters by mouse bone marrow and GC B cells is not entirely coincidental.

The authors are grateful for the excellent technical assistance of J. Przylepa and C. Himes, and for the secretarial skills of R. Frank. We thank Dr. Mario Amzel for his advice and Dr. Jan Cerny for a helpful review of the manuscript.

This work was supported by U.S. Public Health Service grants AI-24335 and AG-10207.

Address correspondence to Garnett Kelsoe, Department of Microbiology and Immunology, University of Maryland School of Medicine, 655 W. Baltimore St., Baltimore, MD 21201.

Received for publication 21 July 1995.

References

1. Kroese, F.G.M., A.S. Wubenna, H.G. Seijen, and P. Nieuwenhuis. 1987. Germinal centers develop oligoclonally. *Eur. J. Immunol.* 17:1069–1072.
2. Jacob, J., R. Kassir, and G. Kelsoe. 1991. In situ studies of the primary immune response to (4-hydroxy-3-nitrophenyl)acetyl. I. The architecture and dynamics of responding cell populations. *J. Exp. Med.* 173:1165–1175.
3. Liu, Y.-J., J. Zhang, P.J.L. Lane, E.Y.T. Chan, and I.C.M. MacLennan. 1991. Sites of specific B cell activation in primary and secondary responses to T cell-dependent and T cell-independent antigens. *Eur. J. Immunol.* 21:2951–2962.
4. Rose, M.L., M.S.C. Birbeck, V.J. Wallis, J.A. Forrester, and A.J.S. Davies. 1980. Peanut lectin binding properties of germinal centres of mouse lymphoid tissue. *Nature (Lond.).* 284: 364–366.
5. Fuller, K., O. Kanagawa, and M.H. Nahm. 1993. T cells within germinal centers are specific for the immunizing antigen. *J. Immunol.* 151:4505–4512.
6. Kelsoe, G., and B. Zheng. 1993. Sites of B cell activation in vivo. *Curr. Opin. Immunol.* 5:418–422.
7. Zheng, B., W. Xue, and G. Kelsoe. 1994. Locus-specific somatic hypermutation in germinal center T cells. *Nature (Lond.).* 372:556–559.
8. Tew, J.G, M.H. Kosco, G.F. Burton, and A.K. Szakal. 1990. Follicular dendritic cells as accessory cells. *Immunol. Rev.* 117: 185–211.
9. Kosco-Vilbois, M.H., D. Gray, D. Scheidegger, and M. Julius. 1993. Follicular dendritic cells help resting B cells to become effective antigen-presenting B cells: induction of B7/BB1 and upregulation of major histocompatibility complex class II molecules. *J. Exp. Med.* 178:2055–2066.
10. Jacob, J., G. Kelsoe, K. Rajewsky, and U. Weiss. 1991. Intraclonal generation of antibody mutants in germinal centers. *Nature (Lond.).* 354:389–392.
11. McHeyzer-Williams, M.G., M.J. McLean, P.A. Labor, and G.V.J. Nossal. 1993. Antigen-driven B cell differentiation in vivo. *J. Exp. Med.* 178:295–307.
12. Küppers, R., M. Zhao, M.L. Hansmann, and K. Rajewsky. 1993. Tracing B cell development in human germinal centers by molecular analysis of single cells picked from histological sections. *EMBO (Eur. Mol. Biol. Organ.) J.* 12:4955–4967.
13. Pascual, V., Y.-J. Liu, A. Magalski, O. deBouteiller, J. Banchereau, and J.D. Capra. 1994. Analysis of somatic mutation in five B cell subsets of human tonsil. *J. Exp. Med.* 180:329–339.
14. Cumano, A., and K. Rajewsky. 1986. Clonal recruitment and somatic mutation in the generation of immunological memory to the hapten NP. *EMBO (Eur. Mol. Biol. Organ.) J.* 5:2459–2468.
15. Berek, C., A. Berger, and M. Apel. 1991. Maturation of the immune response in germinal centers. *Cell.* 67:1121–1129.
16. Weiss, U., and K. Rajewsky. 1990. The repertoire of somatic antibody mutants accumulating in the memory compartment after primary immunization is restricted through affinity maturation and mirrors that expressed in the secondary response. *J. Exp. Med.* 172:1681–1689.
17. Allen, D., T. Simon, F. Sablitzsky, K. Rajewsky, and A. Cumano. 1988. Antibody engineering for the analysis of affinity maturation of an anti-hapten response. *EMBO (Eur. Mol. Biol. Organ.) J.* 7:1995–2001.
18. Kocks, C., and K. Rajewsky. 1988. Stepwise intraclonal maturation of antibody affinity through somatic hypermutation. *Proc. Natl. Acad. Sci. USA.* 85:8206–8210.
19. Makela, O., and K. Karjalainen. 1977. Inherited immunoglobulin idiotypes of the mouse. *Immunol. Rev.* 34:119–138.
20. Reth, M., T. Imanishi-Kari, and K. Rajewsky. 1979. Analysis of the repertoire of anti-NP antibodies in C57BL/6 mice by cell fusion. II. Characterization of idiotypes by monoclonal anti-idiotype antibodies. *Eur. J. Immunol.* 9:1004–1013.
21. Bothwell, A.L.M., M. Paskind, M. Reth, T. Imanishi-Kari, K. Rajewsky, and D. Baltimore. 1981. Heavy chain variable region contribution to the NP^b family of antibodies: somatic mutation evident in the γ2a variable region. *Cell.* 24:625–637.
22. Cumano, A., and K. Rajewsky. 1985. Structure of primary anti-(4-hydroxy-3-nitrophenyl)acetyl (NP) antibodies in nor-

mal and idiotypically suppressed C57BL/6 mice. *Eur. J. Immunol.* 15:512–520.
23. Jacob, J., and G. Kelsoe. 1992. In situ studies of the primary immune response to (4-hydroxy-3-nitrophenyl)acetyl. II. A common clonal origin for periarteriolar lymphoid sheath-associated foci and germinal centers. *J. Exp. Med.* 176:679–687.
24. Jacob, J., J. Przylepa, C. Miller, and G. Kelsoe. 1993. In situ studies of the primary response to (4-hydroxy-3-nitrophenyl)acetyl. III. The kinetics of V region mutation and selection in germinal center B cells. *J. Exp. Med.* 178:1293–1307.
25. Han, S., K. Hathcock, B. Zheng, T.B. Kepler, R. Hodes, and G. Kelsoe. 1995. Cellular interaction in germinal centers. Roles of CD40 ligand and B7-2 in established germinal centers. *J. Immunol.* 155:556–567.
26. McHeyzer-Williams, M.G., G.J. Nossal, and P.A. Lalor. 1991. Molecular characterization of single memory B cells. *Nature (Lond.).* 350:502–505.
27. Hawkins, R.E., and G. Winter. 1992. Cell selection strategies for making antibodies from variable gene libraries: trapping the memory pool. *Eur. J. Immunol.* 22:867–870.
28. Tao, W., F. Hardardottir, and A.L.M. Bothwell. 1993. Extensive somatic mutation in the Ig heavy chain V genes in a late primary anti-hapten immune response. *Mol. Immunol.* 30: 593–602.
29. Miller, C., and G. Kelsoe. 1995. Ig V_H hypermutation is absent in the aged mouse. *J. Immunol.* 155:3377–3384.
30. Diamond, B., and M.D. Scharff. 1994. Somatic mutation of the T15 chain gives rise to an antibody with autoantibody specificity. *Proc. Natl. Acad. Sci. USA.* 81:5841–5844.
31. Shlomchik, M.J., A. Marshak-Rothstein, C.B. Wolfowicz, T.L. Rothstein, and M.G. Weigert. 1987. The role of clonal selection and somatic mutation in autoimmunity. *Nature (Lond.).* 328:805–811.
32. Marion, T.N., D.M. Tillman, and N.-T. Jou. 1990. Interclonal and intraclonal diversity among anti-DNA antibodies from an (NZB × NZW)F1 mouse. *J. Immunol.* 145:2322–2332.
33. Kelsoe, G. 1995. In situ studies of the germinal center reaction. *Adv. Immunol.* 60:267–288.
34. Pulendran, B., G. Kannourakis, S. Nouri, K.G.C. Smith, and G.J.V. Nossal. 1995. Soluble antigen can cause enhanced apoptosis of germinal-centre B cells. *Nature (Lond.).* 375:331–334.
35. Shokat, K.M., and C.C. Goodnow. 1995. Antigen-induced B-cell death and elimination during germinal-centre immune responses. *Nature (Lond.).* 375:334–338.
36. Gavrieli, Y., Y. Sherman, and S.A. Ben-Sasson. 1992. Identification of programmed cell death in situ via specific labeling of nuclear DNA fragmentation. *J. Cell Biol.* 119:493–501.
37. Ravetch, J.V. 1994. Fc receptors: rubor redux. *Cell.* 78:553–560.
38. Pepys, M.B. 1975. Studies in vivo of cobra factor and murine C3. *Immunology.* 28:369–377.
39. Lichtenstein, L.M., and S. Margolis. 1968. Histamine release in vitro: inhibition by catecholamines and methylxanthines. *Science (Wash. DC).* 161:902–903.
40. Bochner, B.S., B.J. Undem, and L.M. Lichtenstein. 1994. Immunological aspects of allergic asthma. *Annu. Rev. Immunol.* 12:295–335.
41. Coico, R.F., S. Boghal, and G.J. Thorbecke. 1983. Relationship of germinal centers in lymphoid tissue to immunologic memory V1. Transfer of B cell memory with lymphnode cells fractionated according to their receptors for peanut agglutinin. *J. Immunol.* 131:2254–2257.
42. Hanna, M.G. 1964. An autoradiographic study of the germinal center in spleen white pulp during early intervals of the immune response. *Lab. Invest.* 13:95–104.
43. Korthanuer, U., D. Graf, H. Mages, F. Brière, P. Munoreedevi, S. Malcolm, A.G. Vgazio, L.D. Notorangelo, R.J. Levinsky, and R.A. Krozek. 1993. Defective expression of T-cell CD40 ligand causes X-linked immunodeficiency with hyper-IgM. *Nature (Lond.).* 361:539–541.
44. van den Eertwegh, A.J.M., R.J. Noelle, M. Roy, D.M. Shepherd, A. Aruffo, J.A. Ledbetter, W.J.A. Boersma, and E. Claasen. 1993. In vivo CD40–gp-39 interactions are essential for thymus-dependent humoral immunity. I. In vivo expression of CD40 ligand, cytokines, and antibody production delineates sites of cognate T-B cell interactions. *J. Exp. Med.* 178:1555–1565.
45. Kepler, T.B., and A.S. Perelson. 1993. Cyclic re-entry of germinal center B cells and the efficiency of affinity maturation. *Immunol. Today.* 14:412–415.
46. Daniel, P.T., and P.H. Kramer. 1994. Activation induces sensitivity toward APO-1 (CD95)-mediated apoptosis in human B cells. *J. Immunol.* 152:5624–5632.
47. Ju, S.-T., H. Cui, D.J. Panka, R. Ettinger, and A. Marshak-Rothstein. 1994. Participation of target Fas protein in apoptosis pathway induced by $CD4^+$ Th1 and $CD8^+$ cytotoxic T cells. *Proc. Natl. Acad. Sci. USA.* 91:4185–4189.
48. Rothstein, T.L., J.K.M. Wang, D.J. Panka, L.C. Foote, Z. Wang, B. Stranger, H. Cui, S. Ju, and A. Marshak-Rothstein. 1995. Protection against Fas-dependent Th1-mediated apoptosis by antigen receptor engagement in B cells. *Nature (Lond.).* 374:163–165.
49. Watanabe-Fukunaga, R., C.I. Brannan, N.G. Copeland, N.A. Jenkins, and S. Nagata. 1992. Lymphoproliferation disorder in mice explained by defects in Fas antigen that mediates apoptosis. *Nature (Lond.).* 356:314–317.
50. Adachi, M., R. Watanabe-Fukunaga, and S. Nagata. 1993. Aberrant transcription caused by the insertion of an early transposable element in an intron of the Fas antigen gene of *lpr* mice. *Proc. Natl. Acad. Sci. USA.* 90:1756–1760.
51. Wu, J., T. Zhou, J. He, and J.D. Mountz. 1993. Autoimmune disease in mice due to integration of an endogenous retrovirus in an apoptosis gene. *J. Exp. Med.* 178:461–468.
52. Liu, Y.-J., D.E. Joshua, G.T. Williams, C.A. Smith, J. Gordon, and I.C.M. MacLennan. 1989. Mechanism of antigen driven selection in germinal centres. *Nature (Lond.).* 342: 929–931.
53. Choi, M.S.K., L.H. Boise, A.B. Gottschalk, J. Quintans, C.B. Thompson, and G.G.B. Klaus. 1995. The role of bcl-x_L in CD40-mediated rescue from anti-μ-induced apoptosis in WEH1-231 B lymphoma cells. *Eur. J. Immunol.* 25:1352–1357.
54. Gu, H., D. Tarlinton, W. Muller, K. Rajewsky, and I. Förster. 1991. Most peripheral B cells in mice are ligand selected. *J. Exp. Med.* 173:1357–1371.
55. Betz, A.G., M.S. Neuberger, and C. Milstein. 1993. Discriminating intrinsic and antigen-selected mutational hotspots in immunoglobulin V genes. *Immunol. Today.* 14:405–411.
56. Allen, D., A. Cumano, R. Dildrop, C. Kocks, K. Rajewsky, N. Rajewsky, J. Ross, F. Sablitzky, and M. Siekevitz. 1987. Timing, genetic requirements and functional consequences of somatic hypermutation during B-cell development. *Immunol. Rev.* 96:5–22.
57. Blier, P.R., and A.L.M. Bothwell. 1988. The immune response to the hapten NP in C57BL/6 mice: insights into the

structure of the B-cell repertoire. *Immunol. Rev.* 105:27–43.
58. Tao, W., and A.L.M. Bothwell. 1990. Development of B cell lineages during a primary anti-hapten immune response. *J. Immunol.* 145:3216–3222.
59. Yuhasz, S.C., C. Parry, M. Strand, and L.M. Amzel. 1995. Structural analysis of affinity maturation: the three-dimensional structures of complexes of an anti-nitrophenol antibody. *Mol. Immunol.* In press.
60. Nagata, S., and P. Golstein. 1995. The Fas death factor. *Science (Wash. DC).* 267:1449–1456.
61. Tartaglia, L.A., T.M. Ayres, G.H.W. Wong, and D.V. Goeddel. 1993. A novel domain within the 55 kd TNF receptor signals cell death. *Cell.* 74:845–853.
62. Golstein, P., D. Marguet, and V. Depraetere. 1995. Homology between reaper and the cell death domains of Fas and TNFR1. *Cell.* 81:185–186.
63. Itoh, N., Y. Tsujimoto, and S. Nagata. 1993. Effect of bcl-2 on Fas antigen-mediated cell death. *J. Immunol.* 151:621–627.
64. Liu, Y.-J., C. Barthélémy, O. de Bouteiller, C. Arpin, I. Durand, and J. Banchereau. 1995. Memory B cells from human tonsils colonize mucosal epithelium and directly present antigen to T cells by rapid up-regulation of B7-1 and B7-2. *Immunity.* 2:239–248.
65. Rathmell, J.C., M.P. Cooke, W.Y. Ho, J. Grein, S.E. Townsend, M.M. Davis, and C.C. Goodnow. 1995. CD95 (Fas)-dependent elimination of self-reactive B cells upon interaction with $CD4^+$ T cells. *Nature (Lond.).* 376:181–183.
66. Nossal, G.J.V. 1983. Cellular mechanisms of immunologic tolerance. *Annu. Rev. Immunol.* 1:33–66.
67. Goodnow, C.C. 1992. Transgenic mice and analysis of B-cell tolerance. *Annu. Rev. Immunol.* 10:489–518.
68. Carsetti, R., G. Köhler, and M.C. Lamers. 1995. Transitional B cells are the target of negative selection in the B cell compartment. *J. Exp. Med.* 181:2129–2140.
69. Reynaud, C.-A., C. Garcia, W.R. Hein, and J.-C. Weil. 1995. Hypermutation generating the sheep immunoglobulin repertoire is an antigen-independent process. *Cell.* 80:115–125.